



# Modeling of an industrial mixing valve and electrostatic coalescer for crude oil dehydration and desalination

Mohammad Shooshtari, Mehdi Karimi, and Mehdi Panahi

Ferdowsi University of Mashhad, Faculty of Engineering, Chemical Engineering Department, Mashhad, Iran

## ABSTRACT

This paper aims to present a new model for an industrial desalination system including a mixing valve and an electrostatic coalescer. This model uses a one-dimensional population balance equation in steady-state conditions. The effect of hydrodynamic, diffusion and electrostatic mechanisms on the collision or breaking of water droplets dispersed in crude oil was considered. Also, using the film drainage model, the droplet coalescence rate has been determined. The developed model can predict the outlet droplet size distribution as well as the desalination and dehydration efficiency. The simulation results showed good agreement with the industrial data. Finally, the effect of some important parameters on the electrostatic desalination process, such as mixing valve pressure drop, electric field intensity, crude oil viscosity, crude oil temperature, diluting water flow rate, and crude oil API on the efficiency of the process was analyzed. The results indicated that by increasing the crude oil temperature from 314 to 334 K, the efficiency of dehydration improves from 97.95% to 99.02%. Also, reducing crude oil API from 33 to 30 and crude oil viscosity from 4 to 2 mPa.s caused a decrease in water separation by 2.88% and 1.16%, respectively.

## ARTICLE HISTORY

Received 4 November 2022  
Accepted 21 February 2023

## KEYWORDS

Mixing valve; population balance; electrostatic coalescer; electric field; droplet

## 1 Introduction

Due to the presence of many impurities such as water and salt in the crude oil extracted from the reservoirs, different methods are used to separate them to improve the quality of crude oil and reduce industrial costs. The most important methods of separating water and salt from crude oil are thermal, gravity, chemical, and electrical methods. The electrical method is one of the common methods in the oil industry to remove water and salt from crude oil.<sup>[1]</sup> The most important parts of the electrostatic coalescer include the oil distributors, electrodes, and power supply. The electric field used in the electrostatic coalescer is divided into three categories according to the type of current: direct (DC), alternating (AC), and the combination of direct and alternating current.<sup>[2]</sup> Many studies and research have been done on the process of separating salt and water from oil. Meidanshahi et al determined the droplet size distribution and salt concentration along the electrostatic coalescer using the two-variable population balance equation.<sup>[3]</sup> Miter et al. presented the breakup and collision functions of droplets with good accuracy for water-in-oil emulsion flow. They also determined the droplet size distribution using the population balance equation.<sup>[4]</sup> Aryafard et al. studied the effect of electric

field intensity and the mixing valve pressure drop in a desalination unit using the population balance equation. The results showed that with the increase in the intensity of the electric field from 2 to 2.5 kV/cm, the dehydration efficiency increases from 96.4% to 97.8%.<sup>[5]</sup> In their model, the effect of crude oil movement on droplet collision was not considered. Mardani et al. investigated the movement and coalescence of drops passing through a channel exposed to an electric field and found that increasing the inlet velocity causes faster coalescence of the droplets.<sup>[6]</sup> Mohammadi et al. presented a numerical model to determine the effect of electric field wave mode and concluded that the square wave has the best efficiency in the process.<sup>[7]</sup> Anand et al. presented a numerical model to find the droplet size distribution in an electrical integration process. They considered the droplets as spherical and assumed that the forces that enter the droplets include only electric and drag forces. Their results showed that increasing the average droplet diameter can increase the dynamics of the coalescence process.<sup>[8]</sup> Bagheri et al modeled the use of electric mixing based on the population balance equation and determined its effect on desalination efficiency. The results showed that replacing the electric mixing system with a mixing

70 valve improves the efficiency of the process.<sup>[9]</sup> Akbarian Kakhki et al. by modifying the model of Aryafard et al. studied the effect of electric field frequency. The results of their modeling indicated that increasing the frequency from 50 to 300 HZ decreases the amount of water in the outlet oil by 0.03%.<sup>[10]</sup> Mousavi et al. investigated the formation of secondary droplets due to partial coalescence. By applying an electric field on the oil-water emulsion, the droplets completely or partially coalesced with each other. They investigated the effect of electric field intensity and interfacial tension on the secondary droplet volume.<sup>[11]</sup> Gong et al. simulated droplet coalescence and separation in the simultaneous presence of electric field and centrifugal motion. In this study, the coalescence model based on turbulence force and electric field is used in the population balance equation. The results showed that increasing the inlet flow rate first increases and then decreases the efficiency of the process.<sup>[12]</sup> Su et al. simulated the performance of electrostatic coalescence in oil-water emulsion based on the population balance equation. In this research, an equation was proposed to calculate the collision efficiency of droplets.<sup>[13]</sup> Yhan et al. modeled the kinetics of droplet coalescence in oil-water emulsion based on the population balance equation. The results of this research showed that reducing the shear rate and the volume ratio of the dispersed phase will increase the droplet coalescence time.<sup>[14]</sup> As mentioned in some research about crude oil desalination, the population balance equation can be used to determine the droplet size distribution as well as the effect of different parameters on it. However, there is no comprehensive model for an industrial electrostatic desalination system that takes into account the different coalescence or breakup mechanisms of water droplets. Therefore, in this work, an industrial electrostatic desalination process will be modeled using the population balance equation.

The main goal of this research is to present a new model based on the one-dimensional population balance equation to determine the droplet size distribution, dehydration, and desalination efficiency in a single-stage industrial crude oil desalination process including a mixing valve and an electrostatic coalescer. In the mixing valve, the effects of the mechanisms of turbulence and Brownian motion, and in the electrostatic coalescer, the effects of the mechanisms of differential sedimentation, laminar shear, Brownian motion, and electric field on the coalescence or breaking of droplets are considered. In the second part, the process of electrostatic dehydration and desalination of crude oil is described. In the third part, the modeling of the mixing valve and the electrostatic coalescer are connected, and the considered assumptions are explained. Finally, in

the fourth part, modeling results and process performance are discussed.

### 1.1 Process description

Usually, a suitable demulsifier is added before starting the dehydration process to reduce the interfacial tension between water and oil.<sup>[15]</sup> After that, the diluent water and crude oil are mixed using a mixing valve until the salt concentration reaches an acceptable level. In the mixing valve, the droplets break under the influence of the turbulent force. In addition to turbulence, the Brownian force causes droplets to collide and coalesce. The diffusion mechanism is important for ultrafine droplets. The emulsion exiting from the mixing valve enters the electrostatic coalescer to start the process of separating water and salt, which flows upwards by the distributors. In the electrostatic coalescer, water droplets dispersed in crude oil are affected by various forces. These forces may cause drops to collide or break. The emulsion entered into the electrostatic coalescer first flows through the section without an electric field so that the larger droplets settle and separate from the crude oil, then it enters the space between the electrodes so that the electric field increases the rate of brine separation from the oil. Therefore, the electrostatic coalescer is divided into two parts. In the first part, gravity, buoyancy, drag, and Brownian forces are applied to the drops. Therefore, Droplets collide with each other under the influence of the mechanisms of differential sedimentation, laminar shear, and diffusion. In the second part, in addition to the forces of the first part, electric forces are also applied to the droplets. In this part, the electric field causes the droplets to be polarized, as a result, a dipole-dipole force between the droplets increases the number of collisions. When small droplets collide with each other, if the collision energy is sufficient, coalescence occurs and larger droplets are formed. If the formed droplets have a suitable weight, the gravitational force overcomes the drag force and the drops settle. [Figure 1](#) shows the single-stage desalination process and [Table 1](#) shows the specification of the flow of crude oil, diluting water, the electrostatic coalescer, and the mixing valve.

## 2 Mathematical modeling of the process

In the present work, among the various mathematical theories that have been used to predict the dispersion of droplets in a continuous phase, the population balance equation method has been selected. This equation is used in various branches of engineering, such as crystallization of liquid-liquid extractors, liquid-liquid phase

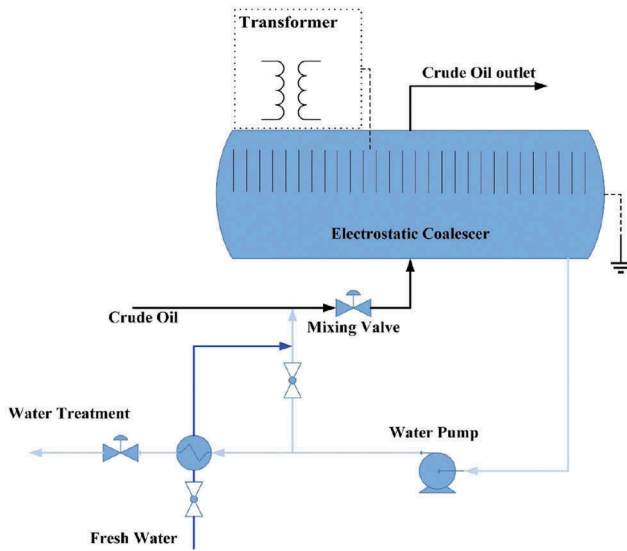


Figure 1. Single-stage electrostatic desalination process.

Table 1. Characteristics of feed, mixing valve and electrostatic coalescer.

Property	Value
Feed	
Crude oil rate (bbl/day)	55000
Crude oil temperature (K)	324
API	33
Water cut (%)	10
Crude oil salt content (PTB)	81.69
Fresh water	
Flow rate	3% of crude oil
Temperature (K)	314
Mixing valve	
Pressure drop (bar)	1.7
Electrostatic coalescer Length (m)	13.72
Diameter (m)	3.05
Electrodes length (m)	0.3
Electrical field (kV/cm)	1.5

systems, agitated continuous phase systems, and generally, every dispersed phase is used in a continuous phase. In this equation, droplet breakage and coalescence, and the change in the droplet size distribution, are investigated. Considering the steady state conditions and moving in one direction ( $z$ ), The population balance equation is defined as follows<sup>[16]</sup>:

$$\begin{aligned}
 u \frac{\partial n(v, z)}{\partial z} = & -g(v)n(v, z) \\
 & + \frac{1}{2} \int_{w=0}^v \beta(v, v-w)n(w, z)n(v-w, z)dw \\
 & + \int_{w=v}^{\infty} f(v, w)g(w)n(w, z)dw \\
 & - n(v, z) \int_{w=0}^{\infty} \beta(v, w)n(w, z)dw
 \end{aligned} \quad (1)$$

On the right-hand side of Eq. 1, the first and fourth terms respectively, show the loss of droplets due to the breaking of droplets and coalescence with other drops.

The second and third terms respectively, demonstrate the formation of droplets due to the coalescence of smaller droplets with each other and the breaking of larger droplets.

## 2.1 Mixing valve modeling

In the mixing valve, by adding diluting water to crude oil, the salt concentration is reduced. Turbulent force is the dominant force for breaking drops. The breakage caused by the turbulent force can be divided into two categories based on the size of the active eddies. Håkanson et al. proposed a breaking frequency with good accuracy by simulating the formation of emulsion under the influence of turbulence:

Smaller eddies than drops act by inertial forces (turbulent inertia)<sup>[17]</sup>:

$$g_1(d) = K_1 \frac{\sqrt{8.2\xi_c^{2/3}d^{2/3} - \frac{8\lambda W_{ecr}}{(\rho_c d)}}}{d} \cdot \frac{\rho_c \xi_c^{1/3} d^{4/3}}{2\mu_d} \quad (2)$$

The eddies larger than the droplet cause the droplet to break with the viscous mechanism (turbulent viscous)<sup>[17]</sup>:

$$g_2(d) = K_2 \frac{\sqrt{16.4\mu_c \xi_c^{1/3} d^{-2/3} / \rho_c - 8\lambda Ca_{cr} / (\rho_c d)}}{d} \cdot \frac{\mu_c}{\mu_d} \quad (3)$$

All droplets are affected by both types of eddies, so the overall breakage function is defined as the sum of breakage functions caused by eddies smaller and larger than drops.

$$g(d) = \begin{cases} g_1(d) + g_2(d) & \text{if } Ca > Ca_{crit} \\ 0 & \text{if } Ca \leq Ca_{crit} \end{cases} \quad (4)$$

$$\xi_c = \frac{\Delta P}{t_{res} \rho_c} \quad (5)$$

$$\lambda = \left( \frac{v_c^3}{\xi_c} \right)^{0.25} \quad (6)$$

Large droplets are more unstable than smaller droplets, so they are more likely to break. The capillary number is a measure of the breaking of droplets, so if it becomes greater than its critical value, the drop will break.

$$Ca_{crit} = \frac{\mu_c d_{crit} \sqrt{\frac{\xi_c}{v_c}}}{2\sigma} \quad (7)$$

$d_{crit}$  is the smallest attainable diameter at the outlet of the mixing valve and is related to the maximum Reynolds number.<sup>[4]</sup> The probability function is used to determine the probability of the formation of a small droplet with the volume of  $v$  from the breaking of a larger droplet with the volume of  $v_0$ .

So far, many probability functions have been proposed by researchers. Considering that the cause of droplet breakage in the mixing valve is turbulence and the droplet breakage is not binary, therefore Raikar et al. proposed the probability distribution function of daughter particles as follows<sup>[18]</sup>:

$$f(v, v_0) = m(m-1) \left(1 - \frac{V}{V_0}\right)^{m-2} \quad (8)$$

Where  $m$  is the number of droplets formed due to the breaking of the larger droplet. Miter et al. experimentally suggested the collision frequency of droplets caused by turbulence as follows<sup>[4]</sup>:

$$\theta^T(i, j) = K_3 \frac{\pi}{8} (d_i + d_j)^3 \sqrt{\frac{\xi_c}{v_c}} \quad (9)$$

Droplets also collide with each other due to the diffusion phenomenon. Brownian force becomes more important for ultrafine droplets. The collision frequency caused by the Brownian force is defined as follows<sup>[19]</sup>:

$$\theta^{Br}(i, j) = \frac{2k_B T}{3\mu_c} (d_j + d_i) \left(\frac{1}{d_j} + \frac{1}{d_i}\right) \quad (10)$$

On the other hand, we know that not all collisions cause droplet merging, so the collision efficiency is defined as follows<sup>[4]</sup>:

$$e_{ij} = \exp \left[ -K_4 \frac{\sqrt{3}}{8} \left(\frac{\mu_d}{\mu_c}\right) Ca_{eq}^{1.5} \left(\frac{d_{eq}}{h_f}\right) \right] \quad (11)$$

where

$$d_{eq} = 2 \left(\frac{1}{d_i} + \frac{1}{d_j}\right)^{-1} \quad (12)$$

$$h_f = \left(\frac{Ad_{eq}}{16\pi\sigma}\right)^{1/3} \quad (13)$$

$\beta$  is equal to the number of collisions that cause a coalescence. Therefore, it is determined by multiplying the sum of collision frequencies caused by turbulent and Brownian forces in the collision efficiency.

$$\beta(d_i, d_j) = (\theta^T + \theta^{Br}) e_{ij} \quad (14)$$

## 2.2 Electrostatic coalescer modeling

After mixing the diluting water and crude oil in the mixing valve, the outlet emulsion enters the electrostatic coalescer. The electric field polarizes the droplets. Therefore, by creating an attractive force between the surfaces of the droplets and increasing the probability of the droplet collisions with each other, droplet coalescence increases. As mentioned, the electrostatic coalescer is divided into two parts. In the first part, the droplets are affected by hydrodynamic and diffusion mechanisms. These forces include gravity, buoyancy, drag, and Brownian. The sum of the forces of gravity and buoyancy causes the tendency of the drops to fall. On the other hand, the drag force created by the flow of crude oil causes the drops to move upwards. Brownian force is also used to take into account the effect of diffusion of the dispersed phase. The electrostatic coalescer is designed in such a way that the rising velocity of crude oil is very low. According to the flow rate of crude oil and the geometry of the electrostatic coalescer, the upward velocity of crude oil is around 1 to 3 mm.s<sup>-1</sup>. Therefore, according to the calculated Reynolds number, the oil flow regime in the electrostatic coalescer is laminar, so, there is no external force that can stress the droplets and cause the droplets to break. In the second part, where the emulsion passes through the electric field, in addition to the forces mentioned in the first part, electric forces are also applied to the droplets. When the induced electric force is greater than the critical value, it can break the droplets and they are broken into smaller droplets. As seen in Fig. 2, the electrostatic coalescer is divided into several elements. Two streams enter and two streams leave each element so that the outlet stream from the upper and lower elements enters the element, and the two outlet streams enter the lower and upper element. In the population balance equation, by having the inlet drops of each element, the outlet drops of each element can be calculated. Drops that reach the diameter necessary for settling are removed from the bottom of the element and other drops from the top of the element. The number of elements is determined in such a way that their further increase does not cause a significant change in the accuracy of calculations.

As was said before, in the electrostatic coalescer, due to the laminar flow of crude oil, the droplet-breaking phenomenon does not occur. But if the electric field exceeds the critical value, it can cause the droplets to break. The critical electric field can be determined from the following equation<sup>[20]</sup>:

$$E_c = 0.64 \sqrt{\frac{\sigma}{\epsilon d}} \quad (15)$$

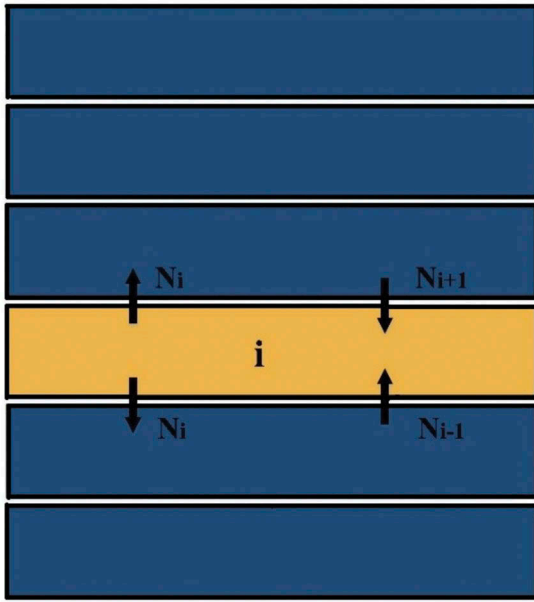


**Figure 2.** The structure of assumed elements for the electrostatic coalescer.

According to Eq. 15, the intensity of the electric field considered in this study is less than the critical value for all droplets. Therefore, the droplet-breaking phenomenon will not occur in the electrostatic coalescer.

290 **2.2.1. Assuming a one-dimensional movement, steady-state conditions, and no breaking of the droplets, the population balance equation is defined as follows: (16)**

$$u \frac{\partial n(v, z)}{\partial z} = \frac{1}{2} \int_{w=0}^v \beta(v, v-w) n(w, z) n(v-w, z) dw - n(v, z) \int_{w=0}^{\infty} \beta(v, w) n(w, z) dw \quad (16)$$

295 As previously mentioned, the rising velocity of crude oil can be determined using the inlet flow rate and the geometry of the electrostatic coalescer.  $u$  in Eq. 11 is the slip velocity, which is obtained from the difference between the crude oil velocity and the droplet settling velocity.

$$u = u_c - \frac{(\rho_d - \rho_c)gd^2}{18\mu_c} \quad (17)$$

300 First, we will describe the coalescence of droplets in the absence of an electric field. The direction of the gravity force is downward and the buoyancy force is upward. As mentioned, the combined forces of gravity and buoyancy make the droplets tend to fall and thus cause the droplets to collide.

Zhang et al presented the following equation for collision frequency caused by the differential sedimentation mechanism<sup>[21]</sup>:

$$\theta^{Ds}(d_i, d_j) = \frac{\pi}{4} (d_i + d_j)^2 V_{ij} \quad (18)$$

$$V_{ij} = \frac{(\mu' + 1) |\rho_d - \rho_c| d_j^2 (1 - \delta^2) g}{6(3\mu' + 2)\mu_c} \quad (19)$$

$$\delta = \frac{d_i}{d_j} \quad d_i \leq d_j \quad (20)$$

The drag force enters the droplets due to the flow of crude oil. The flow rate of crude oil in the electrostatic coalescer is very laminar, Therefore, it can't cause the droplets to break. The collision frequency due to laminar shear proposed by Smoluchowski is defined as follows<sup>[22]</sup>:

$$\theta^{Ls}(d_i, d_j) = \frac{\gamma(d_i + d_j)^3}{6} \quad (21)$$

Where  $\gamma$  is the average shear rate in the electrostatic coalescer.

As it was said in the mixing valve modeling section, the Brownian force can also be a factor in the collision of very small droplets. Therefore, the collision frequency caused by the Brownian motion ( $\theta^{Br}$ ) that was expressed in Eq. 10 is also considered in this part.

320 The film drainage model is used to determine collision efficiency. In this model, the efficiency is obtained based on the droplet contact time and the time required for coalescence<sup>[23]</sup>:

$$e_{ij} = \exp\left(-\frac{t_{ij}}{\tau_{ij}}\right) \quad (22)$$

325 The contact time of two droplets is expressed by the following equation<sup>[24]</sup>:

$$\tau_{ij} \sim \frac{d_{eq}^{2/3}}{\xi_c^{1/3}} \quad (23)$$

Collision efficiency due to the laminar shear mechanism is given by:

$$e_{ij}^{Ls} = \exp\left[-K_5 \left(\frac{\mu_d}{\mu_c}\right) \left(\frac{\mu_c \dot{\gamma} d_{eq}}{\sigma}\right)^{3/2} \left(\frac{8\pi\sigma d_{eq}^2}{A}\right)^{1/3}\right] \quad (24)$$

330 It is worth noting that the efficiency of different collision mechanisms is not the same. But due to the lack of information provided and also the dominance of the laminar shear mechanism, it is assumed that the efficiency of other mechanisms (differential sedimentation

and Brownian motion) is similar to the efficiency of the laminar shear mechanism. Therefore, the following overall integration rate was employed.

$$\beta(d_i, d_j) = (\theta^{Ds} + \theta^{Ls} + \theta^{Br})e_{ij}^{Ls} \quad (25)$$

In the second part of the desalter, in addition to the forces mentioned in the first part, electric forces are also applied to the droplets. Electric forces include dipole-dipole, electrophoretic, and di-electrophoretic. Electrophoretic force is more important in DC field than AC field. Also, the effect of di-electrophoretic force on droplet collisions is insignificant, so the most important electrostatic mechanism is the dipole-dipole force. This force, which is the result of the polarization of the droplets, improves the coalescence rate by increasing the number of collisions.

Atten, by studying the behavior of droplets exposed to an AC electric field, proposed the collision frequency caused by the electric force as follows<sup>[20]</sup>:

$$\theta^E(d_i, d_j) = \frac{\pi}{36} (d_i + d_j)^3 \left( \frac{di}{dj} + \frac{dj}{di} \right) \left( \frac{\epsilon_c E^2}{\mu_c} \right) \quad (26)$$

The characteristic time for electric force has been derived by Atten<sup>[20]</sup>:

$$t_{ij}^E = C \frac{\sqrt{3\mu_c}}{4\phi\epsilon_c E^2} \quad (27)$$

Factors such as natural surfactants in crude oil and demulsifier concentration are effective on the interfacial tension between water and oil. For this reason, the adjustable constant C is determined experimentally to consider the effect of these properties on the coalescence time. By calculating the droplet coalescence rate caused by the electric force, the overall coalescence rate is given by:

$$\beta(d_i, d_j) = (\theta^{Ds} + \theta^{Ls} + \theta^{Br})e_{ij}^{Ls} + \theta^E e_{ij}^E \quad (28)$$

### 3 Numerical solution

There are many methods of solving the population balance equation, such as the method of classes, method of moments, quadrature method of moments, and direct quadrature method of moments. In this study, the method of classes was chosen among various methods to solve the population balance equation. The reason for choosing this method is that it is a simple method with good accuracy and also allows the direct use of particle size classes determined from experimental data without any manipulation. The class method was presented by Kumar and Ramakrishna. In this method, by creating droplet-

size classes, the equation is solved for each class. Then, using the answer of all the classes, the size distribution of the outlet droplets is determined.  $n(v, z)$  is discrete for different classes.  $N_i(z)$  represents the number of the droplets in the  $i^{\text{th}}$  class that their volume is between  $v_i$  and  $v_{i+1}$ <sup>[25]</sup>:

$$N_i(z) = \int_{v_i}^{v_{i+1}} n(v, z) dv \quad (29)$$

Therefore, using the classes method, the population balance equation is defined as follows.:

$$\begin{aligned} u \frac{dN_i(z)}{dz} = & -g_i N_i + \sum_{j \geq k} \left( 1 - \frac{1}{2} \delta_{j,k} \right) \eta \beta_{j,k} N_j N_k \\ & - N_i \sum_{k=1}^M \beta_{i,k} N_k + \sum_{k=i+1}^M n_{i,k} g_k N_k \end{aligned} \quad (30)$$

Where

$$n_{i,k} = \int_{x_i}^{x_{i+1}} \frac{x_{i+1} - v}{x_{i+1} - x_i} f(v, x_k) dv + \int_{x_{i-1}}^{x_i} \frac{v - x_{i-1}}{x_i - x_{i-1}} f(v, x_k) dv \quad (31)$$

$$\eta = \begin{cases} \frac{(x_j + x_k) - x_{i-1}}{x_i - x_{i-1}} & x_{i-1} \leq (x_j + x_k) \leq x_i \\ \frac{x_{i+1} - (x_j + x_k)}{x_{i+1} - x_i} & x_i \leq (x_j + x_k) \leq x_{i+1} \end{cases} \quad (32)$$

$$x_i = 0.5(v_{i-1} + v_i) \quad (33)$$

Considering that the pressure drop of the mixing valve, electric field intensity, crude oil viscosity, crude oil temperature, diluting water flow rate, and crude oil API have a significant effect on the performance of the process of separating water and salt of crude oil. The proposed model can determine the effect of these parameters on desalination and dehydration efficiencies.

### 4 Results and discussion

To determine the droplet size distribution in the oil exiting from the mixing valve and the electrostatic coalescer, 100 droplet size classes with equal size intervals in the range of 0.1–1000  $\mu\text{m}$  are considered as system inlets. Adding more size classes had a negligible effect on increasing the accuracy of the calculations and did not change the simulation results. Therefore, the number of 100-size classes were considered. The simulation results are discussed in three parts, involving model validation, performance analysis of the mixing valve, and AC electrostatic coalescer. The accuracy of the model and its assumptions have been compared with plant data from the South Iran Oil Company.

#### 4.1 Model validation

405 To verify the accuracy of the presented model, the efficiency of dehydration and desalination has been compared with the industrial data. Dehydration efficiency is the amount of water in the oil exiting the electrostatic coalescer compared to the initial amount of it in the crude oil. In the oil industry, PTB is pounds of salt per thousand barrels of oil. Table 2 show the comparison between the modeling results and industrial data. From Table 2, it is clear that the efficiency predicted by the model is in good agreement with the industrial data.

410

415

#### 4.2 Mixing valve

In this part, the mixing valve simulation results are analyzed. As the flow passes through the mixing valve, droplets break due to external stress and smaller droplets are produced, so the emulsion becomes more stable. As it is clear from Fig. 3 the diameter of the incoming droplets is in the range of 0.1–1000  $\mu\text{m}$ . As the emulsion passes through the mixing valve, the number of fine droplets in the outlet crude oil increases.

420

425 Therefore, the pick of size distribution curve has been transferred from the diameter of 350  $\mu\text{m}$  at the inlet feed to the diameter of 140  $\mu\text{m}$  at the outlet flow. Also, droplets with a diameter greater than 390  $\mu\text{m}$  have been removed from the system. Therefore, the main mechanism in the mixing valve is the breaking of droplets caused by the turbulence force.

430

##### 4.2.1 Effect of pressure drop

According to Eq. 5, the pressure drop affects the energy dissipation rate ( $\xi_c$ ). Therefore, an increase in pressure drop increases the energy dissipation rate and as a result, increases the rate of breaking and collision of droplets. But the effect of this parameter on the droplet breaking frequency is much higher. Figure 4 presents the increase in pressure drop from 1.5 to 2 bar, causing an increase in the breaking rate of the droplet and as a result, the number of small droplets grows. large droplets are more unstable than smaller droplets and the probability of their breaking is higher under the influence of external stresses. Therefore, with the increase in the pressure drop, the breaking of larger

435

440

445

**Table 2.** Comparison between simulation results and industrial data at steady state conditions.

	Modeling result	Industrial data
Dehydration efficiency	98.44%	98.54%
Desalination efficiency	94.06%	94.15%
PTB	4.85	4.78

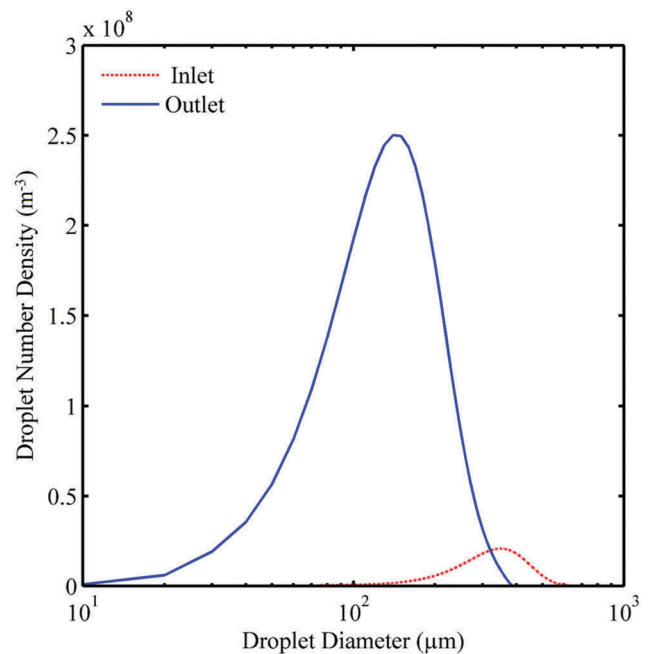


**Figure 3.** Droplet size distribution in inlet and outlet of mixing valve.

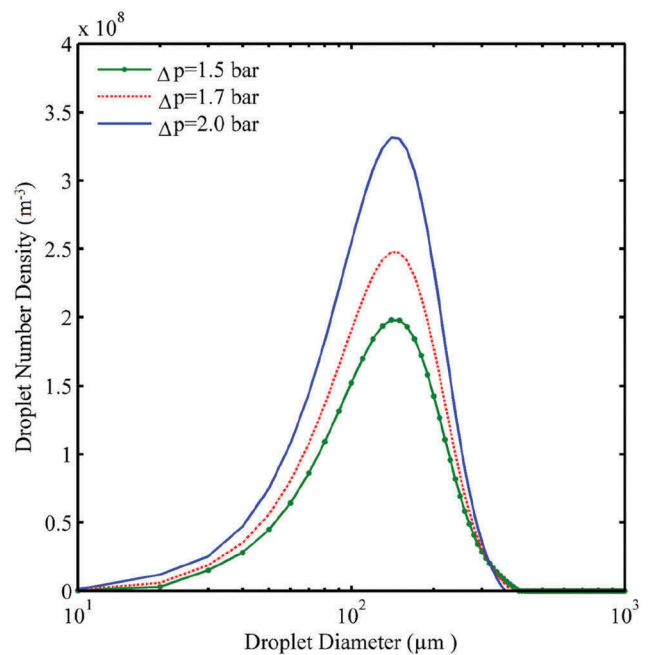


**Figure 4.** The effect of pressure drop on the size distribution of water droplets exiting from the mixing valve.

droplets occurs more often. In addition, increasing the pressure drop has shifted the maximum of the droplet size distribution diagram from 150 to 130  $\mu\text{m}$  in the outlet emulsion. Also, the diameter of the smallest droplet that is removed from the system has been decreased. Increasing the pressure drop makes the

emulsion more stable by increasing the breaking rate of the droplets. Therefore, the separation of water and salt is reduced. Droplet size distribution in the first part of the electrostatic coalescer. Droplet size distribution in the second part of the electrostatic coalescer.

### 4.3 Electrostatic coalescer

In this part, in addition to presenting the simulation results of the electrostatic coalescer, we investigate the effect of some important parameters on the electrostatic desalination process, such as the mixing valve pressure drop, diluting water flow rate, electric field intensity, crude oil viscosity, crude oil temperature, and crude oil API. In this work, the electrostatic coalescer was divided into two parts based on the electric field. The oil entering the electrostatic coalescer is sent upwards by the distributors. Droplet size distribution in the first element of the coalescer is the sum of the drops coming out of the mixing valve and the drops coming from the upper element due to gravitational force. Figure 5(a) indicates the droplet size distribution in different sections of the first 70 cm of the electrostatic coalescer. The droplets collide due to gravity, buoyancy, drag, and Brownian forces. Due to the low coalescence rate of droplets caused by these mechanisms, the effect of this part on the separation of water from oil is not significant. Then the emulsion enters the space between the electrodes and the droplet collision occurs under the influence of electric force in addition to hydrodynamic and diffusion mechanisms. As Fig. 5(b) shows in this part, the dipole-dipole force caused by the electric field increases the drops' collision and coalescence. Larger droplets are formed and settle due to the dominance of gravity over the drag force. Therefore, the separation of water and salt is significantly increased. Finally, the crude oil exits from the top and the separated brine exits from the bottom of the electrostatic coalescer.

#### 4.3.1 Effect of mixing valve pressure drop

As mentioned earlier, the increase in pressure drop in the mixing valve due to the effect on the energy dissipation rate leads to more droplet breakage and as a result, more fine droplets are produced in the mixing valve. With the increase of fine droplets at the outlet of the mixing valve, the frequency of droplet collisions and, as a result, the rate of merging in the electrostatic coalescer decreases. It is clear from Fig. 6 that when the pressure drop of the mixing valve increased from 1.5 to 2 bar, the separation of fine droplets and the dehydration efficiency are reduced. Also, increasing the pressure drop causes better and more mixing of crude oil with fresh water and increases the salt separation efficiency.

Therefore, it is important to determine the optimal pressure drop to achieve optimal desalination and dehydration efficiency. The modeling results showed that if the pressure drop increases from 1.5 to 2 bar, the dehydration efficiency decreases from 98.60% to 98.21%.

#### 4.3.2 Effect of electric field intensity

It is clear that increasing the intensity of the electric field, in addition to increasing the droplet collision frequency, reduces the time required for merging. Therefore, increasing the electric field intensity by increasing the polarization of the drops increases their coalescence rate. On the other hand, with the increase of the coalescence rate, the droplet settles due to the gravitational force and as a result the separation of water and salt increases. If the electric field intensity becomes more than its critical value, droplet breakage will occur and as a result, the efficiency of the process will decrease. As Fig. 7 shows, increasing the electric field intensity from 0.5 to 2.5 kV/cm has shifted the droplet size distribution diagram downward, Also, the number of larger drops that come out with the oil has decreased. Therefore, the volume of water in the outlet oil has decreased significantly, so the dehydration efficiency has increased from 97.76% to 99.16%.

#### 4.3.3 Effect of crude oil viscosity

Table 3 shows the value of dehydration and desalination efficiency in three different viscosity. Although the temperature is the most important parameter affecting viscosity, other parameters such as wax content, oil concentration, etc. also affect crude oil viscosity. Reducing the viscosity of crude oil is effective in increasing the settling velocity of droplets. The force of resistance to the movement of water droplets approaching each other is known as the film thinning force. This force is mainly dependent on the viscosity of crude oil, so the decrease in viscosity causes a decrease in the resistance force against collision and the coalescence of droplets. Therefore, as the droplet coalescence increases, the efficiency of the process increases. The simulation results indicated that by reducing the viscosity of crude oil from 4 to 2 mPa.s, water separation efficiency increased by 1.16%.

#### 4.3.4 Effect of crude oil temperature

As the crude oil temperature increases, Brownian motion and natural displacement increase. Therefore, the possibility of droplet collision increases. On the other hand, changing the solubility of the demulsifier causes more instability of the emulsion. Also, an increase in temperature leads to a decrease in the viscosity of crude oil and increases the settling velocity of

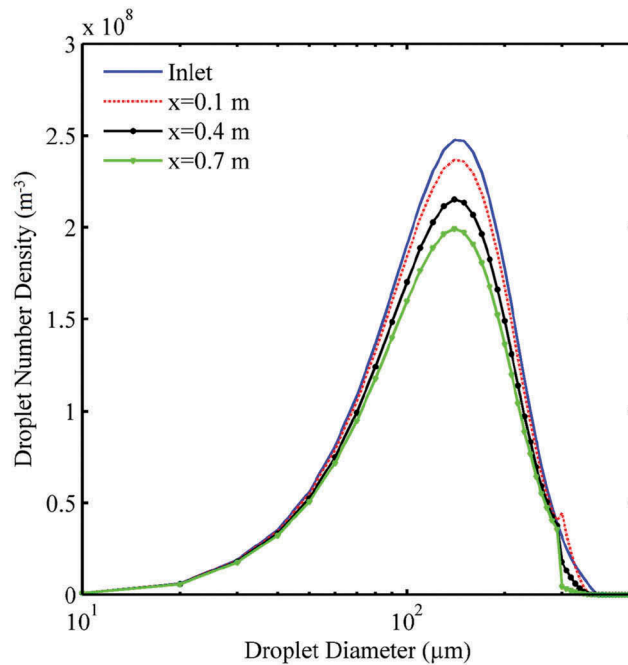


Figure 5a. Droplet size distribution in the first part of the electrostatic coalescer.

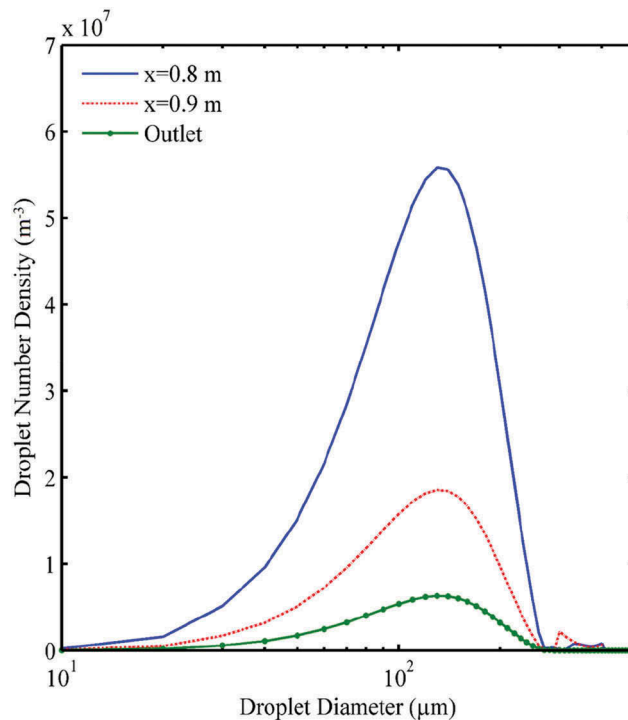


Figure 5b. Droplet size distribution in the second part of the electrostatic coalescer.

555 droplets, so more droplets settle. As Fig. 8 shows, by increasing the oil temperature from 314 to 334 K, the minimum diameter required for sedimentation decreased, as a result, the dehydration efficiency increased from 97.95% to 99.02%. Also, temperature changes did not affect droplets with a diameter of less than 60  $\mu\text{m}$ . Therefore, the crude oil temperature

changes have been more effective in the distribution of larger droplets than fine droplets. If the temperature is too high, by reducing the density difference of water and oil, the settling velocity of the droplets decreases, it also reduces the interfacial tension of water droplets and causes them to break and produce smaller droplets, as a result, the efficiency of the process decreases.

560

565

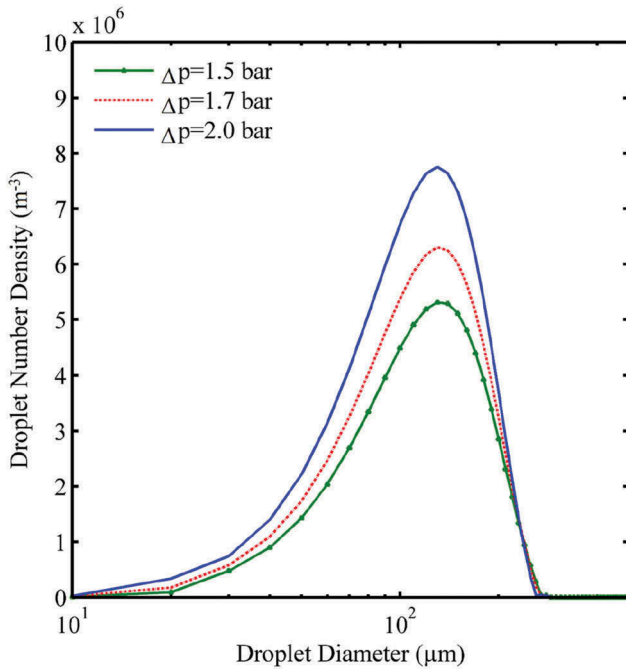


**Figure 6.** The effect of the mixing valve pressure drop on the droplet size distribution exiting the electrostatic coalescer.

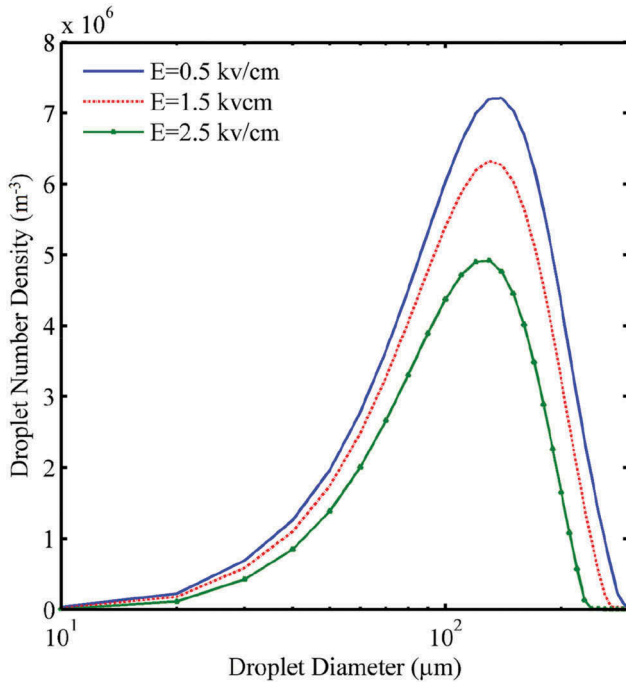


**Figure 7.** The effect of the electric field intensity on the droplet size distribution exiting the electrostatic coalescer.

#### 4.3.5 Effect of diluting water flow rate

Injecting water into the water-oil emulsion causes the concentration of salt to be diluted and the salt crystals and sediments present in the oil to dissolve. **Figure 9** shows the distribution of droplets in oil leaving the system at two diluting water flow rates. Although the

**Table 3.** Effect of crude oil viscosity on dehydration and desalination efficiency.

Crude oil viscosity (mPa.s)	2	3	4
Dehydration efficiency	99.22%	98.44%	98.06%
Desalination efficiency	94.80%	94.06%	93.71%
PTB	4.25	4.85	5.14

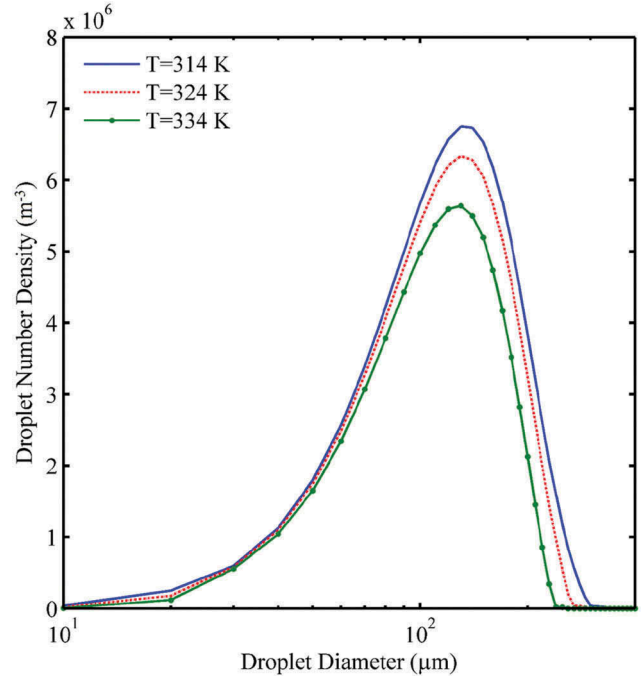


**Figure 8.** The effect of the oil temperature on the droplet size distribution exiting the electrostatic coalescer.

increase in the flow rate of diluting water has caused an increase in the number of fine droplets in the outlet oil, on the other hand, the collision and coalescence of droplets increase. Therefore, the production rate of larger droplets and their removal due to the gravitational force has increased. Increasing the diluting water too much will increase the amount of outlet water and as a result more salt. With the increase in the diluting water flow rate from 3% to 5%, the efficiency of desalination and dehydration has increased by 0.69% and 3.07%, respectively.

#### 4.3.6 Effect of crude oil API

**Figure 10** shows the effect of crude oil API reduction on droplet distribution. As the API of crude oil decreases, the oil specific gravity increases, which causes the density difference between water and oil to decrease. Therefore, the droplet settling velocity decreases according to Stokes' law and water separation becomes more difficult. Also, due to the lower amount of asphaltene in light oils than in heavy oils, the oil layer around the droplets breaks more easily and causes more

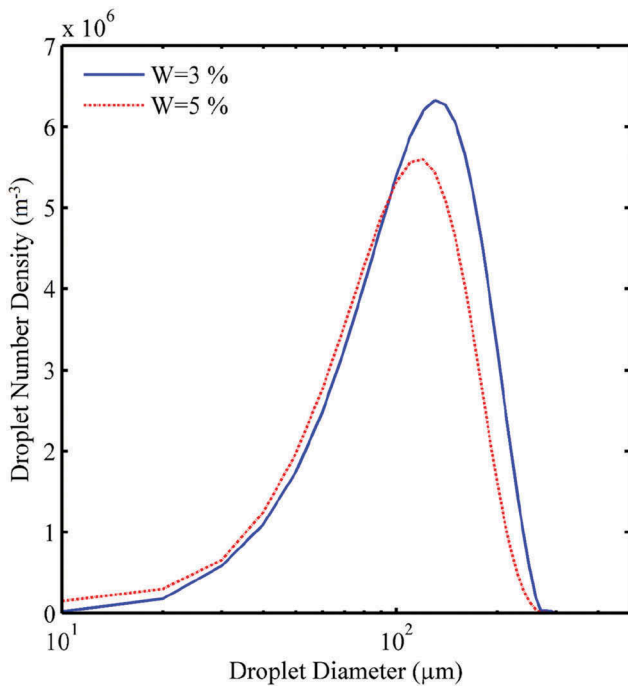


**Figure 9.** The effect of the diluting water rate on the droplet size distribution exiting the electrostatic coalescer.

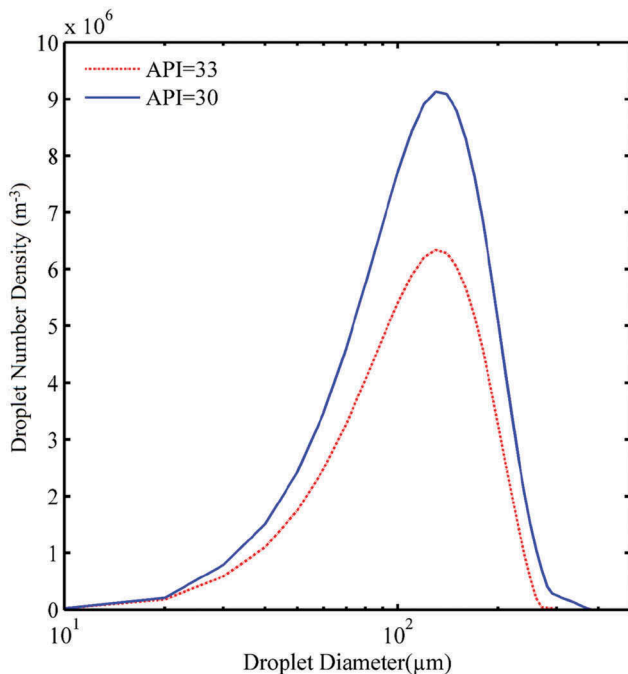


**Figure 10.** The effect of the crude oil API on the droplet size distribution exiting the electrostatic coalescer.

from 98.44% to 95.56%. The efficiency of the process decreases significantly as the crude oil becomes heavier. To solve this problem, it is suggested to increase the flow rate of diluting water and increase the concentration of suitable demulsifier to reduce the interfacial tension between the water and oil. 600

## 5 Conclusion

In this study, using the population balance method, the industrial desalination system including a mixing valve and an electrostatic coalescer with a horizontal electric field was modeled. In this model, hydrodynamic, diffusion, and electrostatic aspects that cause droplets to coalesce, or break were considered. Finally, using the developed model, the size distribution of droplets in the outlet oil from the electrostatic coalescer and the efficiency of the process were determined. To verify the accuracy of the model, the obtained results were compared with industrial data. Then, the effect of mixing valve pressure drop, electric field intensity, crude oil viscosity, crude oil temperature, diluting water flow rate, and crude oil API on the droplet size distribution, dehydration, and desalination efficiencies in the desalination process was studied. The obtained results indicated that: increasing the mixing valve pressure drop from 1.5 to 2 bar reduces water separation by 0.4%. 605  
Increasing the electric field intensity from 0.5 to 2.5 kV/cm by increasing the dipole-dipole force between the drops causes an increase in the number of effective droplet collisions. Therefore, the efficiency of dehydration increased from 97.76% to 99.16%. Also, increasing the oil temperature from 314 to 334 K has increased the droplet settling velocity, as a result of which, the dehydration efficiency has increased from 97.95% to 99.02%. 610  
The simulation results showed that by reducing the viscosity of crude oil from 4 to 2 mPa.s, while increasing the droplet settling velocity, the water separation efficiency increases by 1.16% due to the reduction of the film thinning force. As the dilution water flow rate increases from 3% to 5% due to increased droplet collision and coalescence, the dehydration efficiency increases from 98.44% to 99.13%. As the API of the crude oil decreases, the droplet settling velocity decreases, so smaller droplets cannot settle. Also, due to the increase of interfacial tension between water and oil, reduces the collision efficiency. For this reason, by reducing the API of crude oil from 33 to 30, the separation of water from crude oil is reduced by 2.88%. 615  
620  
625  
630  
635  
640

640  
645  
650  
655  
660  
665  
670  
675  
680  
685  
690  
695  
700  
705  
710  
715  
720  
725  
730  
735  
740  
745  
750  
755  
760  
765  
770  
775  
780  
785  
790  
795  
800  
805  
810  
815  
820  
825  
830  
835  
840  
845  
850  
855  
860  
865  
870  
875  
880  
885  
890  
895  
900  
905  
910  
915  
920  
925  
930  
935  
940  
945  
950  
955  
960  
965  
970  
975  
980  
985  
990  
995  
1000  
1005  
1010  
1015  
1020  
1025  
1030  
1035  
1040  
1045  
1050  
1055  
1060  
1065  
1070  
1075  
1080  
1085  
1090  
1095  
1100  
1105  
1110  
1115  
1120  
1125  
1130  
1135  
1140  
1145  
1150  
1155  
1160  
1165  
1170  
1175  
1180  
1185  
1190  
1195  
1200  
1205  
1210  
1215  
1220  
1225  
1230  
1235  
1240  
1245  
1250  
1255  
1260  
1265  
1270  
1275  
1280  
1285  
1290  
1295  
1300  
1305  
1310  
1315  
1320  
1325  
1330  
1335  
1340  
1345  
1350  
1355  
1360  
1365  
1370  
1375  
1380  
1385  
1390  
1395  
1400  
1405  
1410  
1415  
1420  
1425  
1430  
1435  
1440  
1445  
1450  
1455  
1460  
1465  
1470  
1475  
1480  
1485  
1490  
1495  
1500  
1505  
1510  
1515  
1520  
1525  
1530  
1535  
1540  
1545  
1550  
1555  
1560  
1565  
1570  
1575  
1580  
1585  
1590  
1595  
1600  
1605  
1610  
1615  
1620  
1625  
1630  
1635  
1640  
1645  
1650  
1655  
1660  
1665  
1670  
1675  
1680  
1685  
1690  
1695  
1700  
1705  
1710  
1715  
1720  
1725  
1730  
1735  
1740  
1745  
1750  
1755  
1760  
1765  
1770  
1775  
1780  
1785  
1790  
1795  
1800  
1805  
1810  
1815  
1820  
1825  
1830  
1835  
1840  
1845  
1850  
1855  
1860  
1865  
1870  
1875  
1880  
1885  
1890  
1895  
1900  
1905  
1910  
1915  
1920  
1925  
1930  
1935  
1940  
1945  
1950  
1955  
1960  
1965  
1970  
1975  
1980  
1985  
1990  
1995  
2000  
2005  
2010  
2015  
2020  
2025  
2030  
2035  
2040  
2045  
2050  
2055  
2060  
2065  
2070  
2075  
2080  
2085  
2090  
2095  
2100  
2105  
2110  
2115  
2120  
2125  
2130  
2135  
2140  
2145  
2150  
2155  
2160  
2165  
2170  
2175  
2180  
2185  
2190  
2195  
2200  
2205  
2210  
2215  
2220  
2225  
2230  
2235  
2240  
2245  
2250  
2255  
2260  
2265  
2270  
2275  
2280  
2285  
2290  
2295  
2300  
2305  
2310  
2315  
2320  
2325  
2330  
2335  
2340  
2345  
2350  
2355  
2360  
2365  
2370  
2375  
2380  
2385  
2390  
2395  
2400  
2405  
2410  
2415  
2420  
2425  
2430  
2435  
2440  
2445  
2450  
2455  
2460  
2465  
2470  
2475  
2480  
2485  
2490  
2495  
2500  
2505  
2510  
2515  
2520  
2525  
2530  
2535  
2540  
2545  
2550  
2555  
2560  
2565  
2570  
2575  
2580  
2585  
2590  
2595  
2600  
2605  
2610  
2615  
2620  
2625  
2630  
2635  
2640  
2645  
2650  
2655  
2660  
2665  
2670  
2675  
2680  
2685  
2690  
2695  
2700  
2705  
2710  
2715  
2720  
2725  
2730  
2735  
2740  
2745  
2750  
2755  
2760  
2765  
2770  
2775  
2780  
2785  
2790  
2795  
2800  
2805  
2810  
2815  
2820  
2825  
2830  
2835  
2840  
2845  
2850  
2855  
2860  
2865  
2870  
2875  
2880  
2885  
2890  
2895  
2900  
2905  
2910  
2915  
2920  
2925  
2930  
2935  
2940  
2945  
2950  
2955  
2960  
2965  
2970  
2975  
2980  
2985  
2990  
2995  
3000  
3005  
3010  
3015  
3020  
3025  
3030  
3035  
3040  
3045  
3050  
3055  
3060  
3065  
3070  
3075  
3080  
3085  
3090  
3095  
3100  
3105  
3110  
3115  
3120  
3125  
3130  
3135  
3140  
3145  
3150  
3155  
3160  
3165  
3170  
3175  
3180  
3185  
3190  
3195  
3200  
3205  
3210  
3215  
3220  
3225  
3230  
3235  
3240  
3245  
3250  
3255  
3260  
3265  
3270  
3275  
3280  
3285  
3290  
3295  
3300  
3305  
3310  
3315  
3320  
3325  
3330  
3335  
3340  
3345  
3350  
3355  
3360  
3365  
3370  
3375  
3380  
3385  
3390  
3395  
3400  
3405  
3410  
3415  
3420  
3425  
3430  
3435  
3440  
3445  
3450  
3455  
3460  
3465  
3470  
3475  
3480  
3485  
3490  
3495  
3500  
3505  
3510  
3515  
3520  
3525  
3530  
3535  
3540  
3545  
3550  
3555  
3560  
3565  
3570  
3575  
3580  
3585  
3590  
3595  
3600  
3605  
3610  
3615  
3620  
3625  
3630  
3635  
3640  
3645  
3650  
3655  
3660  
3665  
3670  
3675  
3680  
3685  
3690  
3695  
3700  
3705  
3710  
3715  
3720  
3725  
3730  
3735  
3740  
3745  
3750  
3755  
3760  
3765  
3770  
3775  
3780  
3785  
3790  
3795  
3800  
3805  
3810  
3815  
3820  
3825  
3830  
3835  
3840  
3845  
3850  
3855  
3860  
3865  
3870  
3875  
3880  
3885  
3890  
3895  
3900  
3905  
3910  
3915  
3920  
3925  
3930  
3935  
3940  
3945  
3950  
3955  
3960  
3965  
3970  
3975  
3980  
3985  
3990  
3995  
4000  
4005  
4010  
4015  
4020  
4025  
4030  
4035  
4040  
4045  
4050  
4055  
4060  
4065  
4070  
4075  
4080  
4085  
4090  
4095  
4100  
4105  
4110  
4115  
4120  
4125  
4130  
4135  
4140  
4145  
4150  
4155  
4160  
4165  
4170  
4175  
4180  
4185  
4190  
4195  
4200  
4205  
4210  
4215  
4220  
4225  
4230  
4235  
4240  
4245  
4250  
4255  
4260  
4265  
4270  
4275  
4280  
4285  
4290  
4295  
4300  
4305  
4310  
4315  
4320  
4325  
4330  
4335  
4340  
4345  
4350  
4355  
4360  
4365  
4370  
4375  
4380  
4385  
4390  
4395  
4400  
4405  
4410  
4415  
4420  
4425  
4430  
4435  
4440  
4445  
4450  
4455  
4460  
4465  
4470  
4475  
4480  
4485  
4490  
4495  
4500  
4505  
4510  
4515  
4520  
4525  
4530  
4535  
4540  
4545  
4550  
4555  
4560  
4565  
4570  
4575  
4580  
4585  
4590  
4595  
4600  
4605  
4610  
4615  
4620  
4625  
4630  
4635  
4640  
4645  
4650  
4655  
4660  
4665  
4670  
4675  
4680  
4685  
4690  
4695  
4700  
4705  
4710  
4715  
4720  
4725  
4730  
4735  
4740  
4745  
4750  
4755  
4760  
4765  
4770  
4775  
4780  
4785  
4790  
4795  
4800  
4805  
4810  
4815  
4820  
4825  
4830  
4835  
4840  
4845  
4850  
4855  
4860  
4865  
4870  
4875  
4880  
4885  
4890  
4895  
4900  
4905  
4910  
4915  
4920  
4925  
4930  
4935  
4940  
4945  
4950  
4955  
4960  
4965  
4970  
4975  
4980  
4985  
4990  
4995  
5000  
5005  
5010  
5015  
5020  
5025  
5030  
5035  
5040  
5045  
5050  
5055  
5060  
5065  
5070  
5075  
5080  
5085  
5090  
5095  
5100  
5105  
5110  
5115  
5120  
5125  
5130  
5135  
5140  
5145  
5150  
5155  
5160  
5165  
5170  
5175  
5180  
5185  
5190  
5195  
5200  
5205  
5210  
5215  
5220  
5225  
5230  
5235  
5240  
5245  
5250  
5255  
5260  
5265  
5270  
5275  
5280  
5285  
5290  
5295  
5300  
5305  
5310  
5315  
5320  
5325  
5330  
5335  
5340  
5345  
5350  
5355  
5360  
5365  
5370  
5375  
5380  
5385  
5390  
5395  
5400  
5405  
5410  
5415  
5420  
5425  
5430  
5435  
5440  
5445  
5450  
5455  
5460  
5465  
5470  
5475  
5480  
5485  
5490  
5495  
5500  
5505  
5510  
5515  
5520  
5525  
5530  
5535  
5540  
5545  
5550  
5555  
5560  
5565  
5570  
5575  
5580  
5585  
5590  
5595  
5600  
5605  
5610  
5615  
5620  
5625  
5630  
5635  
5640  
5645  
5650  
5655  
5660  
5665  
5670  
5675  
5680  
5685  
5690  
5695  
5700  
5705  
5710  
5715  
5720  
5725  
5730  
5735  
5740  
5745  
5750  
5755  
5760  
5765  
5770  
5775  
5780  
5785  
5790  
5795  
5800  
5805  
5810  
5815  
5820  
5825  
5830  
5835  
5840  
5845  
5850  
5855  
5860  
5865  
5870  
5875  
5880  
5885  
5890  
5895  
5900  
5905  
5910  
5915  
5920  
5925  
5930  
5935  
5940  
5945  
5950  
5955  
5960  
5965  
5970  
5975  
5980  
5985  
5990  
5995  
6000  
6005  
6010  
6015  
6020  
6025  
6030  
6035  
6040  
6045  
6050  
6055  
6060  
6065  
6070  
6075  
6080  
6085  
6090  
6095  
6100  
6105  
6110  
6115  
6120  
6125  
6130  
6135  
6140  
6145  
6150  
6155  
6160  
6165  
6170  
6175  
6180  
6185  
6190  
6195  
6200  
6205  
6210  
6215  
6220  
6225  
6230  
6235  
6240  
6245  
6250  
6255  
6260  
6265  
6270  
6275  
6280  
6285  
6290  
6295  
6300  
6305  
6310  
6315  
6320  
6325  
6330  
6335  
6340  
6345  
6350  
6355  
6360  
6365  
6370  
6375  
6380  
6385  
6390  
6395  
6400  
6405  
6410  
6415  
6420  
6425  
6430  
6435  
6440  
6445  
6450  
6455  
6460  
6465  
6470  
6475  
6480  
6485  
6490  
6495  
6500  
6505  
6510  
6515  
6520  
6525  
6530  
6535  
6540  
6545  
6550  
6555  
6560  
6565  
6570  
6575  
6580  
6585  
6590  
6595  
6600  
6605  
6610  
6615  
6620  
6625  
6630  
6635  
6640  
6645  
6650  
6655  
6660  
6665  
6670  
6675  
6680  
6685  
6690  
6695  
6700  
6705  
6710  
6715  
6720  
6725  
6730  
6735  
6740  
6745  
6750  
6755  
6760  
6765  
6770  
6775  
6780  
6785  
6790  
6795  
6800  
6805  
6810  
6815  
6820  
6825  
6830  
6835  
6840  
6845  
6850  
6855  
6860  
6865  
6870  
6875  
6880  
6885  
6890  
6895  
6900  
6905  
6910  
6915  
6920  
6925  
6930  
6935  
6940  
6945  
6950  
6955  
6960  
6965  
6970  
6975  
6980  
6985  
6990  
6995  
7000  
7005  
7010  
7015  
7020  
7025  
7030  
7035  
7040  
7045  
7050  
7055  
7060  
7065  
7070  
7075  
7080  
7085  
7090  
7095  
7100  
7105  
7110  
7115  
7120  
7125  
7130  
7135  
7140  
7145  
7150  
7155  
7160  
7165  
7170  
7175  
7180  
7185  
7190  
7195  
7200  
7205  
7210  
7215  
7220  
7225  
7230  
7235  
7240  
7245  
7250  
7255  
7260  
7265  
7270  
7275  
7280  
7285  
7290  
7295  
7300  
7305  
7310  
7315  
7320  
7325  
7330  
7335  
7340  
7345  
7350  
7355  
7360  
7365  
7370  
7375  
7380  
7385  
7390  
7395  
7400  
7405  
7410  
7415  
7420  
7425  
7430  
7435  
7440  
7445  
7450  
7455  
7460  
7465  
7470  
7475  
7480  
7485  
7490  
7495  
7500  
7505  
7510  
7515  
7520  
7525  
7530  
7535  
7540  
7545  
7550  
7555  
7560  
7565  
7570  
7575  
7580  
7585  
7590  
7595  
7600  
7605  
7610  
7615  
7620  
7625  
7630  
7635  
7640  
7645  
7650  
7655  
7660  
7665  
7670  
7675  
7680  
7685  
7690  
7695  
7700  
7705  
7710  
7715  
7720  
7725  
7730  
7735  
7740  
7745  
7750  
7755  
7760  
7765  
7770  
7775  
7780  
7785  
7790  
7795  
7800  
7805  
7810  
7815  
7820  
7825  
7830  
7835  
7840  
7845  
7850  
7855  
7860  
7865  
7870  
7875  
7880  
7885  
7890  
7895  
7900  
7905  
7910  
7915  
7920  
7925  
7930  
7935  
7940  
7945  
7950  
7955  
7960  
7965  
7970  
7975  
7980  
7985  
7990  
7995  
8000  
8005  
8010  
8015  
8020  
8025  
8030  
8035  
8040  
8045  
8050  
8055  
8060  
8065  
8070  
8075  
8080  
8085  
8090  
8095  
8100  
8105  
8110  
8115  
8120  
8125  
8130  
8135  
8140  
8145  
8150  
8155  
8160  
8165  
8170  
8175  
8180  
8185  
8190  
8195  
8200  
8205  
8210  
8215  
8220  
8225  
8230  
8235  
8240  
8245  
8250  
8255  
8260  
8265  
8270  
8275  
8280  
8285  
8290  
8295  
8300  
8305  
8310  
8315  
8320  
8325  
8330  
8335  
8340  
8345  
8350  
8355  
8360  
8365  
8370  
8375  
8380  
8385  
8390  
8395  
8400  
8405  
8410  
8415  
8420  
8425  
8430  
8435  
8440  
8445  
8450  
8455  
8460  
8465  
8470  
8475  
8480  
8485  
8490  
8495  
8500  
8505  
8510  
8515  
8520  
8525  
8530  
8535  
8540  
8545  
8550  
8555  
8560  
8565  
8570  
8575  
8580  
8585  
8590  
8595  
8600  
8605  
8610  
8615  
8620  
8625  
8630  
8635  
8640  
8645  
8650  
8655  
8660  
8665  
8670  
8675  
8680  
8685  
8690  
8695  
8700  
8705  
8710  
8715  
8720  
8725  
8730  
8735  
8740  
8745  
8750  
8755  
8760  
8765  
8770  
8775  
8780  
8785  
8790  
8795  
8800  
8805  
8810  
8815  
8820  
8825  
8830  
8835  
8840  
8845  
8850  
8855  
8860  
8865  
8870  
8875  
8880  
8885  
8890  
8895  
8900  
8905  
8910  
8915  
8920  
8925  
8930  
8935  
8940  
8945  
8950  
8955  
8960  
8965  
8970  
8975  
8980  
8985  
8990  
8995  
9000  
9005  
9010  
9015  
9020  
9025  
9030  
9035  
9040  
9045  
9050  
9055  
9060  
9065  
9070  
9075  
9080  
9085  
9090  
9095  
9100  
9105  
9110  
9115  
9120  
9125  
9130  
9135  
9140  
9145  
9150  
9155  
9160  
9165  
9170  
9175  
9180  
9185  
9190  
9195  
9200  
9205  
9210  
9215  
9220  
9225  
9230  
9235  
9240  
9245  
9250  
9255  
9260  
9265  
9270  
9275  
9280  
9285  
9290  
9295  
9300  
9305  
9310  
9315  
9320  
9325  
9330  
9335  
9340  
9345  
9350  
9355  
9360  
9365  
9370  
9375  
9380  
9385  
9390  
9395  
9400  
9405  
9410  
9415  
9420  
9425  
9430  
9435  
9440  
9445  
9450  
9455  
9460  
9465  
9470  
9475  
9480  
9485  
9490  
9495  
9500  
9505  
9510  
9515  
9520  
9525  
9530  
9535  
9540  
9545  
9550  
9555  
9560  
9565  
9570  
9575  
9580  
9585  
9590  
9595  
9600  
9605  
9610  
9615  
9620  
9625  
9630  
9635  
9640  
9645  
9650  
9655  
9660  
9665  
9670  
9675  
9680  
9685  
9690  
9695  
9700  
9705  
9710  
9715  
9720  
9725  
9730  
9735  
9740  
9745  
9750  
9755  
9760  
9765  
9770  
9775  
9780  
9785  
9790  
9795  
9800  
9805  
9810  
9815  
9820  
9825  
9830  
9835  
9840  
9845  
9850  
9855  
9860  
9865  
9870  
9875  
9880  
9885  
9890  
9895  
9900  
9905  
9910  
9915

**Nomenclature**

	A	Hamker coefficient [J]
645	C	Adjustable parameter [-]
	Ca	Capillary number [-]
	d	Droplet diameter [m]
	$e_{ij}$	Collision efficiency [-]
	E	Electric field intensity [ $Vm^{-1}$ ]
650	f(v,w)	Daughter drop size distribution function [-]
	g	acceleration Gravity [ $m s^{-2}$ ]
	g(d)	Breakage frequency [ $s^{-1}$ ]
	K	Adjustable parameter [-]
	$k_B$	Boltzmann's constant [ $J K^{-1}$ ]
655	m	The number of droplets formed per breakage of a droplet [-]
	n(v,z)	Continuous number density [ $m^{-3}$ ]
	Ni(z)	Discrete number density [ $m^{-3}$ ]
	P	Pressure [Pa]
660	$t_{res}$	Resident time [s]
	T	Temperature [K]
	u	Velocity [ $ms^{-1}$ ]
	v	Droplet volume [ $m^3$ ]
	$V_{ij}$	The relative velocity [ $ms^{-1}$ ]
665	w	Droplet volume [ $m^3$ ]
	We	Weber number [-]
	z	Length [m]

**Greek symbols**

	$\beta$	Coalescence rate [ $m^3 s^{-1}$ ]
670	$\gamma$	Shear rate [ $s^{-1}$ ]
	$\delta$	The ratio of small drop diameter to large drop diameter [-]
	$\epsilon$	Permittivity [ $F m^{-1}$ ]
	$\theta$	Collision frequency [ $s^{-1}$ ]
675	$\lambda$	Kolmogorov length scale [m]
	$\mu$	Dynamic viscosity [Pa s]
	$\mu'$	Dynamic viscosity ratio of water and oil [-]
	$\nu$	Kinematic viscosity [ $m^2 s^{-1}$ ]
	$\xi$	Rate of energy dissipation [ $m^2 s^{-3}$ ]
680	$\rho$	Density [ $kg m^{-3}$ ]
	$\sigma$	Interfacial tension [ $N m^{-1}$ ]
	$\tau$	Contact time [s]
	$\varphi$	Water fraction in emulsion [-]

**Superscript**

685	Br	Brownian force
	E	Electric force
	Ds	Differential sedimentation
	Ls	Laminar shear
	T	Turbulent force

**Subscripts**

690	i, j, k	Class number index
	c	Continuous phase
	d	Dispersed phase
	eq	Equivalent

**Research highlights**

- A new model for an integrated mixing valve with an electrostatic coalescer in an industrial plant is presented.
- The simultaneous effect of the mechanisms of differential sedimentation, laminar shear, Brownian motion, and

electric force on the droplet coalescence rate in the electrostatic coalescer was considered. 700

- The high accuracy of the model has been confirmed in comparison with industrial data.
- The effect of important parameters such as the degree of API, viscosity, and temperature of crude oil on the electrostatic desalination process has been investigated. 705

**Acknowledgments**

The research of the corresponding author is supported by a grant from Ferdowsi University of Mashhad (N. 3/58374)

**Disclosure statement**

No potential conflict of interest was reported by the author(s). 710

Q3

**Funding**

The authors reported there is no funding associated with the work featured in this article.

**Statement of Novelty**

- A new model for an integrated mixing valve with an electrostatic coalescer in an industrial plant is presented. 715
- The simultaneous effect of the mechanisms of differential sedimentation, laminar shear, Brownian motion, and electric force on the droplet coalescence rate in the electrostatic coalescer was considered.
- The high accuracy of the model has been confirmed in comparison with industrial data. 720
- The effect of important parameters such as the degree of API, viscosity, and temperature of crude oil on the electrostatic desalination process has been investigated.

**References**

- [1] Kim, B.; Moon, J.; Sung, T.; Yang, S.; Kim, J. Demulsification of Water-In-Crude Oil Emulsions by a Continuous Electrostatic Dehydrator. *Sep. Sci. Tech.* 2002, 37(1307), 1320. DOI: 10.1088/0953-2048/15/9/308. 730
- [2] Eow, J. S. Electrostatic Enhancement of Coalescence of Water Droplets in Oil: A Review of the Technology. *Chem. Eng. J.* 2002, 85(357), 368. DOI: 10.1016/S1385-8947(01)00250-9. 735
- [3] Meidanshahi, V.; Jahanmiri, A.; Rahimpour, M. R. Modeling and Optimization of Two Stage AC Electrostatic Desalter. *Sep. Sci. Tech.* 2012, 47(30), 42. DOI: 10.1080/01496395.2011.614316.
- [4] Mitre, J. F.; Lage, P. L.; Souza, M. A.; Silva, E.; Barca, L. F.; Moraes, A. O.; Coutinho, R. C.; Fonseca, E. F. Droplet Breakage and Coalescence Models for the Flow of Water-In-Oil Emulsions 740

- Through a Valve-Like Element. *Chem. Eng. Res. Des.* **2014**, *92*(2493), 2508. DOI: [10.1016/j.cherd.2014.03.020](https://doi.org/10.1016/j.cherd.2014.03.020).
- 745 [5] Aryafard, E.; Farsi, M.; Rahimpour, M. R.; Raeissi, S. Modeling Electrostatic Separation for Dehydration and Desalination of Crude Oil in an Industrial Two-Stage Desalting Plant. *J. Tai. Ins. Chem. Eng.* **2016**, *58*(141), 147. DOI: [10.1016/j.jtice.2015.06.028](https://doi.org/10.1016/j.jtice.2015.06.028).
- 750 [6] Mardani, M. R.; Ganji, D. D.; Hosseinzadeh, K. Numerical Investigation of Droplet Coalescence of Saltwater in the Crude Oil by External Electric Field. *J. Mol. Liq.* **2021**, *346*. DOI: [10.1016/j.molliq.2021.117111](https://doi.org/10.1016/j.molliq.2021.117111).
- 755 [7] Mohammadi, M.; Shahhosseini, S.; Bayat, M. Numerical Prediction of the Electrical Waveform Effect on Electrocoalescence Kinetic. *Chem. Eng. Res. Des.* **2013**, *91* (904), 918. DOI: [10.1016/j.cherd.2012.09.002](https://doi.org/10.1016/j.cherd.2012.09.002).
- 760 [8] Anand, V.; Patel, R.; Naik, V. M.; Juvekar, V. A.; Thaokar, R. M. Modelling and Particle-Based Simulation of Electro-Coalescence of a Water-In-Oil Emulsion. *J. Comp. Chem. Eng.* **2019**, *121*(608), 617. DOI: [10.1016/j.compchemeng.2018.12.003](https://doi.org/10.1016/j.compchemeng.2018.12.003).
- 765 [9] Bagheri, H.; Ghader, S.; Hosseinpour, F. Application of Electric Mixing Method to Increase Industrial Crude Oil Dehydration Efficiency. *J. Chem. Pet. Eng.* **2021**, *551* (99), 115.
- 770 [10] Akbarian Kakhki, N.; Farsi, M.; Rahimpour, M. R. Effect of Current Frequency on Crude Oil Dehydration in an Industrial Electrostatic Coalescer. *J. Tai. Ins. Chem. Eng.* **2016**, *67*, 1–10. DOI: [10.1016/j.jtice.2016.06.021](https://doi.org/10.1016/j.jtice.2016.06.021).
- 775 [11] Mousavi, S. H.; Shariaty-Niassar, M.; Bahmanyar, H.; Moosavian, M. A. Electrocoalescence of an Aqueous Droplet at an Oil–Water Interface with an Investigation of Secondary Droplets Formation. *Iran. J. Chem. Eng.* **2013**, *10*(30), 44.
- 780 [12] Gong, H.; Li, W.; Zhang, X.; Peng, Y.; Yu, B.; Mou, Y. Simulation of the Coalescence and Breakup of Water-In-Oil Emulsion in a Separation Device Strengthened by Coupling Electric and Swirling Centrifugal Fields. *Sep. Purif. Tech.* **2019**, *238*, 116397. DOI: [10.1016/j.seppur.2019.116397](https://doi.org/10.1016/j.seppur.2019.116397).
- 785 [13] Su, X.; Yang, X.; Yu, Y.; Gao, F.; Wang, X. A Simulation Approach to Predict Electrostatic Coalescence Performance of Water-In-Oil Emulsion Using Population Balance Model. *Sep. Sci. Tech.* **2022**, *58*(538), 550. DOI: [10.1080/01496395.2022.2131577](https://doi.org/10.1080/01496395.2022.2131577).
- [14] Yhan O'neil, W.; Nelmary, R.; Gieberth, R.; Andrea, V.; Jhoa, N. T. Modeling Droplet Coalescence Kinetics in Microfluidic Devices Using Population Balances. *Che. Eng. Sci.* **2019**, *201*(475), 483. DOI: [10.1016/j.ces.2019.02.040](https://doi.org/10.1016/j.ces.2019.02.040). 790
- [15] Nikkhah, M.; Tohidian, T.; Rahimpour, M. R.; Jahanmiri, A. Efficient Demulsification of Water-In-Oil Emulsion by a Novel Nano Titania Modified Chemical Demulsifier. *Chem. Eng. Res. Des.* **2015**, *94* (164), 172. DOI: [10.1016/j.cherd.2014.07.021](https://doi.org/10.1016/j.cherd.2014.07.021). 795
- [16] Ramkrishna, D. *Population Balances, Theory and Applications to Particulate Systems in Engineering*; Academic Press: London, **2000**. 800
- [17] Håkansson, A.; Trägårdh, C.; Bergenståhl, B. Dynamic Simulation of Emulsion Formation in a High-Pressure Homogenizer. *Chem. Eng. Sie.* **2009**, *64*(12), 2925. DOI: [10.1016/j.ces.2009.03.034](https://doi.org/10.1016/j.ces.2009.03.034). 805
- [18] Raikar, N.; Bhatia, S.; Malone, M.; McClements, D.; Almeida-Rivera, C.; Bongers, P.; Henson, M. Prediction of Emulsion Drop Size Distributions with Population Balance Equation Models of Multiple Drop Breakage. *Colloid. Sur.* **2010**, *361*(1–3), 108. DOI: [10.1016/j.colsurfa.2010.03.020](https://doi.org/10.1016/j.colsurfa.2010.03.020). 810
- [19] Friedlander, S. K. *Smoke, Dust, and Haze (Fundamentals of Aerosol Dynamics)*, second ed.; Oxford University Press: New York and Oxford, **2000**.
- [20] Atten, P. Electrocoalescence of Water Droplets in an Insulating Liquid. *J. Electrostatics.* **1993**, *30*(259), 270. DOI: [10.1016/0304-3886\(93\)90080-Q](https://doi.org/10.1016/0304-3886(93)90080-Q). 815
- [21] Zhang, X.; Davis, R. H. The Rate of Collisions Due to Brownian or Gravitational Motion of Small Drops. *J. Fluid. Mech.* **1991**, *230*(479), 504. DOI: [10.1017/S0022112091000861](https://doi.org/10.1017/S0022112091000861). 820
- [22] Smoluchowski, M. Versuch einer mathematischen Theorie der Koagulationskinetik kolloider Lösungen. *Zeitschrift für physikalische chemie (Leipzig)*. **1917**, *92* (124), 168. DOI: [10.1515/zpch-1918-9209](https://doi.org/10.1515/zpch-1918-9209). 825
- [23] Coulaloglou, C. A. (1975) Dispersed phase interactions in an agitated flow vessel. Ph.D. Dissertation, Illinois Institute of Technology, Chicago.
- [24] Levich, V. G. *Physicochemical Hydrodynamics*; Prentice Hall Englewood Cliff, NJ, **1962**. 830
- [25] Kumar, S.; Ramkrishna, D. On the Solution of Population Balance Equations by Discretization-I. A Fixed Pivot Technique. *J. Chem. Eng. Sci.* **1996**, *51*(1311), 1332. DOI: [10.1016/0009-2509\(96\)88489-2](https://doi.org/10.1016/0009-2509(96)88489-2). Q5